A Dissertation on

ROLE OF HETEROATOMS ON CYLINDRICAL CNT SURFACE WITH HEMISPHERICAL TIP

Submitted in the partial fulfillment of the requirements of the degree of

MASTER OF TECHNOLOGY

In

NUCLEAR SCIENCE & ENGINEERING (NSE)

By

NEHA UPADHYAY

2K14/NSE/16

Under the Guidance of

Prof. S. C. Sharma

(Supervisor)

Department of Applied Physics,

Delhi Technological University

(Formerly Delhi College of Engineering)

Govt. of NCT of Delhi

Main Bawana Road, Delhi-110042

JULY 2016

Department of Applied Physics

Delhi Technological University (DTU)

(Formerly Delhi College of Engineering, DCE)

Govt. of NCT of Delhi

Bawana Road, Delhi-110042

CERTIFICATE

*This is to certify that the Major project (AP-811) report entitled "***ROLE OF HETEROATOMS ON CYLINDRICAL CNT SURFACE WITH HEMISPHERICAL TIP***" is a bonafide work carried out by* **Ms. Neha Upadhyay** *bearing Roll No.* **2K14/NSE/16**, *a student of Delhi Technological University, in partial fulfilment of the requirements for the award of Degree in* **Master of Technology** *in* "**Nuclear Science & Engineering**" **(NSE).**

As per declaration of the student this work has not been submitted to any University/ Institute for the award of any Degree/ Diploma.

(**Prof. S. C. SHARMA**)

Supervisor

Head,Department of Applied Physics,

Delhi Technological University,

Delhi-110042

DECLARATION

I declare that this written submission represents my ideas in my own words and where others' ideas or words have been included, I have adequately cited and referenced the original sources. I also declare that I have adhered to all principles of academic honesty and integrity and have not misrepresented or fabricated or falsified any idea/data/fact/source in my submission. I understand that any violation of the above will be cause for disciplinary action by the Institute and can also evoke penal action from the sources which have thus not been properly cited or from whom proper permission has not been taken when needed.

PLACE: NEHA UPADHYAY

DATE: (2K14/NSE/16)

ACKNOWLEDGEMENT

Every work accomplished is a pleasure- a sense of satisfaction. However a number of people always motivate, criticize and appreciate a work with their objective ideas and opinions, hence I'd like to thank all, who have directly or indirectly helped me accomplished this project.

Firstly I would like to thank my project supervisor ***Prof. S. C. Sharma*** *without whose support this project could not be started in first place. Prof. Sharma, who took keen interest in my project, and guided me along until the completion of the project providing all necessary information.*

I am also thankful to ***Ms. Neha Gupta*** *and* ***Mr. Ravi Gupta (Research scholars)*** *for their valuable support and guidance in carrying out this project.*

I am deeply grateful to ***Dr. Nitin Kumar Puri*** *(Assistant Professor and Branch coordinator, NSE) for his support and encouragement in carrying out this project.*

I am also thankful to my other teachers, classmates and department staff for their constant support and encouragements.

Neha Upadhyay

TABLE OF CONTENTS

LIST OF FIGURES

LIST OF SYMBOLS

$k_B = Boltzmann's\ costant = 1.23 \times 10^{-23} m^2 Kg s^{-2} K^{-1}$

$\lambda_d = Debye's\ length$

$e = charge\ of\ the\ electron = 1.60217662 \times 10^{-19}$ coulombs

$m_e = mass\ of\ electron = 9.1 \times 10^{-31} Kg$

$\varepsilon_0 = permitivity\ in\ free\ space = 8.85418782 \times 10^{-12} \mathrm{m^{-3}\ kg^{-1}\ s^4\ A^2}$

$Q = charge\ over\ entire\ CNT\ surface(i.e., hemispherical\ tip\ and\ cylindrical\ surface)$

$n_e = number\ density\ of\ electron$

$n_{iA}, n_{iB}, n_{iC} = number\ density\ of\ type\ A, B, C\ ions, respectively$

$n_A, n_B, n_C = number\ density\ of\ type\ A, B, C\ neutral\ atoms, respectively$

$r_{CNT} = CNT\ tip\ radius$

$h_{CNT} = height\ of\ cylindrical\ surface\ of\ CNT$

$V_s = surface\ potential\ on\ the\ cylindrical\ surface\ of\ CNT$

$T_e = electron\ temperature$

$T_s = substrate\ temperature$

$T_n = neutral\ atom\ temperature$

$T_i = ion\ temperature$

$U_s = substrate\ bias$

ABSTRACT

This project puts forward a theoretical model to examine the growth of the carbon nanotube (CNT) on top of catalyst substrate surface subjected to reactive plasma. Various processes have been considered in this model, such as the charging rate of the CNT, kinetics of electron, ions and neutral atoms. Also, the growth of the CNT due to diffusion and accumulation of ions on the catalyst nanoparticles is taken into account. For characteristic glow discharge plasma, numerical calculation on the impact of ion density, temperature and the substrate bias over the growth rate of carbon nanotubes has been carried out. Through it, the change in radius, height and the number density of hydrocarbon ions with time has been shown. Comparison has been made between the two doped gases that are nitrogen and boron, and also with the undoped condition. Along with it, the change in the concentration of the hydrocarbon ions in plasma along the time is computed for three conditions (undoped, nitrogen doped and boron doped). The CNT considered here has hemi-spherical tip as it provides better field emission which distinguish this work from the work of Tewari and Sharma [31]. Different gases have been used in the process. The mixture of gases includes hydrocarbon (CH_3), hydrogen (H_2), nitrogen (N_2) and boron (B). It is obtained that the height of CNT increments with the number density of carbon ions and radius of CNT reduces with hydrogen ion density. The nitrogen and boron acts as doping elements here. It is found that nitrogen obstruct both the height as well as radius of CNT, whereas in boron, both the radius and height increases in comparison to the nitrogen doping. The present work can serve to the better comprehension of procedure parameters amid growth of **hemispherical tip CNT with cylindrical surface** by a Plasma Enhanced Chemical Vapor Deposition (PECVD) method.

CHAPTER I

1. INTRODUCTION

Carbon nanotubes have fascinated enthusiasm among researchers since they were discovered. Due to their excellent physical and electronic properties, in addition with their chemical inertness, make them promisingly helpful for applications as vast as electron-field emitters, nanoelectrodes, material for scanning microscopy, electrochemical storage devices, fuel cells, etc. They have high aspect ratio, high field emission characteristics, high surface area, and excellent current stability.

Carbon nanotubes can be synthesized in various ways. Some of them are arc discharge method, laser ablation method, chemical vapor deposition and so on. Here, in the present work the growth of carbon nanotubes is done in the presence of plasma through Plasma Enhanced Chemical Vapor Decomposition (PECVD) process. Plasma is considered as it is advantageous over other methods. In plasma the incident particle has high energy due to ionization as compared to neutral atoms in other processes. This increased energy provides high particle reactivity, control of the surface reactivity. Hence the CNTs produced by this process have improved structure, crystallinity and ordering [26].

In the presence of plasma a silicon substrate is taken in a stainless steel cylindrical reactor. On this substrate a layer of catalyst is laid. Here the catalyst used is nickel. Then a mixture of gases including hydrocarbon, hydrogen, nitrogen and boron is introduced in the chamber. The plasma ionizes the various gases present in the chamber to form mixture of ions, electrons, and neutral atoms. Hence multiple species are present which ionize, combine, and dissociate continually to form new species through various chemical reactions. These active species dissociate the catalyst particle to form nanoparticles on which the accretion of carbon atom takes place and hence the carbon nanotubes grow.

A theoretical model is developed for the CNT growth in plasma having different gases. The nitrogen and boron introduced act as the heteroatoms (i.e., doping elements) in the growth of CNT. The model is explained through various processes such as the charging of CNT, balanced equations of electron density, positively charged ions and neutral atoms. The growth rate

equations are also considered here. The CNT presented in this model has hemi-spherical tip with cylindrical curved surface.

Numerical simulation of the model is done and the comparison is shown through the graphs plotted. Among the four gases present, hydrocarbon provides carbon atoms which accretes on the catalyst nanonoparticle to develop CNT, hydrogen is used for the etching of CNT and the effect of nitrogen and boron is that it impacts both the height and the radius of the carbon nanotubes. When compared with each other both these gases have different effects on the structure of CNT. These effects have been shown along with the undoped condition. Also, the effect on the concentration of the hydrocarbon (CH_3 taken here) is presented.

CHAPTER II

2. CARBON NANOTUBES (CNT)

2.1 Carbon Nanotubes (CNT)

Over the few decades, we have seen the discovery, progress and, in a few cases the manufacturing and production of materials which can be said to come under a very small scale or in other words are at nanolevels. These materials are produced on a large scale. Such nanomaterials are comprised of inorganic or organic matter [1]. Carbon Nanotubes (CNTs), graphene, buckyballs, graphite and diamond are the structural arrangements of carbon atom. These structural variations depend on the hybridization found in the arrangement. Graphene is the arrangement of carbon atoms in planer form having sp^2 hybridization. CNTs are one-dimensional cylinders having sp^2 hybridized atoms. They also contain some percentage of sp^3 hybridized atoms which depends on radius of curvature of nanotubes. Nowadays carbon nanotubes (CNTs) and graphene have become one of the most intensively studied nanostructures due to their prominent structural and electrical properties [2-4]. CNT is a hollow cylindrical one dimensional carbon nanostructure. It has high electrical conductivity, large specific surface area, excellent mechanical strength and flexibility. CNTs are very strong, even stronger than steel. If we compare both we can say CNTs are 100 times stronger. Despite of its high strength they are very light, one-sixth the weight of steel. Hence, these nanofibres can be used to fortify any material [5]. Heat and electricity can conduct better by nanotubes than copper. To enhance the conductivity CNTs are used in polymers. Due to strong bonding among the atoms CNTs are only one of its kind and hence are very strong. Despite of its thinness (i.e. a few nanometers), it can be as long as hundreds of microns.

Carbon nanotubes have different structures based on the changing in length, thickness, and number of layers. How a grapheme sheet is rolled up to make CNT can affect their characteristics, hence making it either metal or semiconductor. The graphite layer that forms the nanotube seems as rolled-up chicken wire with a constant unbroken hexagonal mesh. On the apex of these hexagons are carbon molecules.

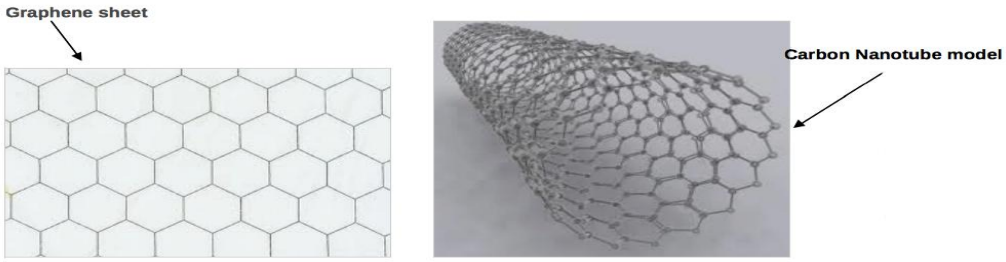

Fig1: Schematic of carbon nanotube made from rolled graphene sheet

[CNT technology overview - http://www.nanoscience.com/applications/education/overview/cnt-technology-overview/]

2.2 Types of Carbon Nanotubes (CNT)

There are mainly two types of CNTS. They are:

(1) Single-walled carbon nanotube (SWNT) structure
(2) Multi-walled carbon nanotube (MWNT) structure

2.2.1 Single-walled carbon nanotube structure

There are three different shapes of single-walled carbon nanotubes. They are:

(1) Armchair
(2) Chiral and
(3) Zigzag

Fig 2:Types of single-walled carbon nanotube

[Scarselli, M, P. Castrucci, and M. De Crescenzi. "Electronic and optoelectronic nano-devices based on carbon nanotubes." *Journal of Physics: Condensed Matter"* **24.31** (2012): 313202]

As the graphene is rolled up into a cylinder, that decides the shapes of the carbon nanotubes. For example, we can imagine the rolling of sheet of a paper from its corners, hence it gives us one of the shapes but when we roll the paper from its edges then it gives the other shape. A figure of single walled nanotube is given below where the chiral vector (n,m) is defined.

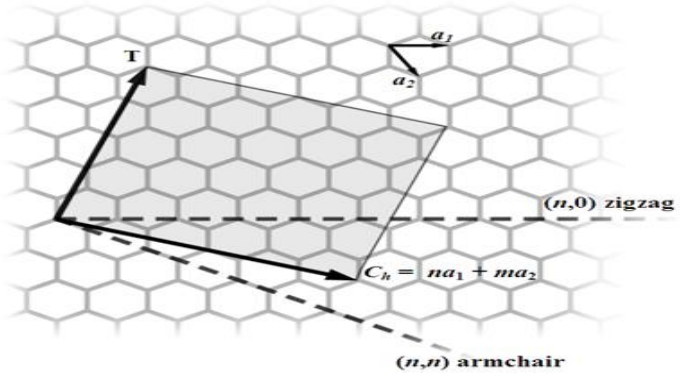

Fig 3: SWCNT represented by a pair of indices (n,m) called the chiral vector

[Optical Investigation of Suspended Single Wall Carbon Nanotubes by David Lakatos, Budapest University of Technology and Economics]

Nanotube's electrical properties are directly affected by the structural design. The nanotube is said to be metallic (i.e. highly conducting) when n-m is a multiple of 3, else it is a semiconductor. Here among the three shapes, Armchair is always metallic whereas other shapes make it a semiconductor.

2.2.2 Multi-walled carbon nanotube structure

Multi-walled nanotubes have two structure models. In the first model which is called Russian Doll model, in which the carbon nanotube consists of concentric ring like structure having two rings in which the outer nanotube has larger diameter than that of inner nanotube. In the second model called as the Parchment model, instead of two grapheme sheets a single graphene sheet is rolled multiple times around itself which resembles like a scroll of paper which has been rolled up. The properties of multi-walled carbon nanotubes is similar to that of single-walled carbon nanotube, but it has an advantage over single-walled carbon nanotubes, that is its outer layers of nanotubes protects the inner layers from any outer chemical interactions. Also, these have higher tensile strength than that of single-walled carbon nanotubes.

2.3 Properties of Carbon nanotubes

The electrical, thermal, and mechanical properties of CNT's are due to the atomic arrangement of carbon atoms. Some of the properties are discussed below [6].

2.3.1 Electrical Conductivity

Metallic CNT are profoundly conductive materials. Chirality, the measure of twist of graphene sheet, decides the conductivity of CNT interconnects. Contingent upon the chiral indices, CNTs show either metallic or semiconducting properties. The electrical conductivity of MWNTs is very complex as their inter-wall communications non-consistently circulate the current over individual tubes. In any case, a uniform distribution of current is seen across various parts of metallic SWNT. Electrodes are put to determine the conductivity and resistivity of various parts of SWNT rope. The calculated resistivity of the SWNT ropes is in the order of 10^{-4} Ω cm at 27 ºC, showing SWNT ropes to be the most conductive carbon fibres. It has been accounted for that an individual SWNT may contain deformities that permits the SWNT to act as a transistor.

2.3.2 Strength and Elasticity

Every carbon atom in a solitary sheet of graphite is associated by means of strong chemical bond to three neighboring atoms. Accordingly, CNTs can show the most grounded basal plane elastic modulus and subsequently are relied upon to be an extreme high quality fiber. The elastic modulus of SWNTs is much higher than steel that makes them profoundly resistant. Nanotube will bend when its tip is pressed; the nanotube comes back to its original state when the force is removed. This property makes CNTs greatly valuable as probe tips for high resolution scanning probe microscopy. Although, the present Young's modulus of SWNT is around 1 TPa, yet a much higher estimation of 1.8 TPa has likewise been accounted for. For various trial estimation procedures, the estimations of Young's modulus vary in the scope of 1.22 TPa – 1.26 TPa relying upon the size and chirality of the SWNTs. It has been seen that the elastic modulus of MWNTs is not emphatically subjected to the diameter. Principally, the moduli of MWNTs are corresponded to the measure of deformities in the nanotube walls.

2.3.3 Thermal Conductivity and Expansion

CNTs can show superconductivity beneath 20 K (roughly −253 ºC) due to the solid in-plane C–C obligations of graphene. The solid C-C bond gives the extraordinary quality and firmness against axial strains. Besides, the bigger interplane and zero in-plane thermal increment of SWNTs results in high adaptability against non-hub strains. Because of their high thermal conductivity and substantial in-plane development, CNTs show energizing prospects in nanoscale molecular electronics, detecting and actuating devices, strengthening additive fibers in functional composite materials, and so on. Recent estimations recommend that the CNT implanted matrices are more grounded in contrast with exposed polymer lattices. In this way, it is normal that the nanotube may likewise altogether enhance the thermo-mechanical and the thermal properties of the composite materials.

2.3.4 Field Emission

Tunneling of electrons from metal tip to vacuum results in field emission phenomenon due to use of strong electric field. Field discharge results from the high perspective proportion and small diameter of CNTs. The field emitters are reasonable for the application in flat-panel displays. For MWNTs, the field discharge properties happen because of the emission of electrons and light. Without connected potential, the luminescence and light emission happens through the electron field emission and visible part of the spectrum, respectively.

2.3.5 Aspect Ratio

High aspect ratio is one of the exciting properties of CNTs, to obtain similar electrical conductivity; a lower CNT load is required. The high aspect ratio of CNTs has remarkable electrical conductivity in contrast with the conventional additive materials, for example, choped carbon fiber, carbon black, or stainless steel fiber.

2.3.6 Absorbent

Due to light weight, higher adaptability, high mechanical strength and predominant electrical properties, carbon nanotubes and CNT composites have been flourishing as absorbing materials.

Subsequently, CNTs develop out as perfect possibility for use in gas, air and water filtration. The absorption frequency range of SWNT-polyurethane composites extends from 6.4–8.2 (1.8 GHz) to 7.5–10.1 (2.6 GHz) and to 12.0–15.1 GHz (3.1 GHz). A considerable measure of research has as of now been completed for replacing the activated charcoal with CNTs for certain ultrahigh purity applications.

2.4 Production of CNTs

Various methods are utilized to deliver CNTs and fullerenes. In prior days, fullerenes were manufactured by vaporizing graphite with a short-pulse, high-power laser strategy, while CNTs were produced by carbon combustion and vapor deposition processes. Utilizing the prior technique (plasma arcing) of creating CNTs in sensible amounts, an electric current was given across two carbonaceous electrode in an inert gas. The plasma arcing strategy is principally used to deliver fullerenes and CNTs from various carbonaceous materials, for example, graphite. The CNTs are deposited on the electrode, while the fullerenes show up in the sediment. Plasma arcing technique can likewise be applied within the presence of cobalt with 3% or more concentration. Distinctive techniques for creation of CNTs are talked about underneath.

2.4.1 Arc Discharge Method

The most widely recognized and simplest approach to fabricate CNTs is the carbon arc discharge method. Utilizing this technique, a composite mixture of components is created that isolates the CNTs from soot and the catalytic metals. Arc vaporization is utilized to create CNTs by putting two carbon bars from end to end, isolated by an approximate separation of 1 mm, kept in an enclosure. At low pressure, the enclosure is filled with inert gas. A high temperature release between two electrode is made by applying a DC of 50 to 100 A. Due to the high temperature discharge, the surface of the carbon electrode is vaporized and a small rod shaped electrode is formed. The manufacture of CNTs in high yield fundamentally relies on upon the consistency of

the plasma arc. CNTs can also be produced by arc discharge method with liquid nitrogen.

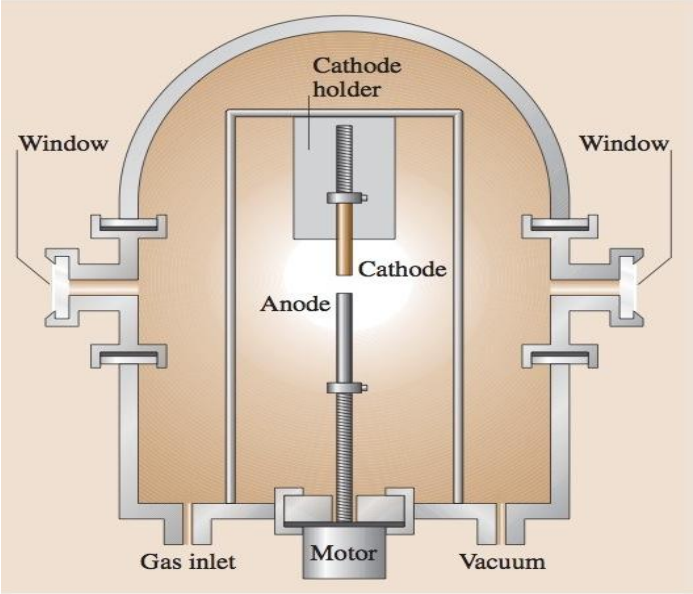

Fig 4: Laser Discharge Method

[H.W. Kroto, J.R. Heath, S.C.O'Brien, R.F. Curl, R.E. Smalley, Nature **318**, 162-163 (1985)]

2.4.2 Laser Method

In 1996, a dual-pulsed laser was utilized as a part of synthesizing systems for manufacturing CNTs with 70% transparency. Now-a-days, the laser vaporization procedure is utilized for producing CNTs. In this procedure, a graphite rod with 50:50 catalyst blends of cobalt and nickel at 1200 °C in flowing argon is utilized to for preparing the sample. The uniform vaporization of the objective can be accomplished by utilizing the initial laser vaporization pulse succeeds by a second pulse. The quantity of deposition of carbon as residue is fundamentally minimized by the utilization of these two progressive laser pulses. The bigger particles are broken by applying the second laser pulse. The CNTs manufactured by this procedure are 10–20 nm in diameter and 100 µm or more long. The usual nanotube measurement and size distribution can shift for various growth temperature, catalyst composition, and different procedure parameters. In the last few years, the arc discharge and laser vaporization strategies are utilized to get top notch CNTs in little amount. Nonetheless, both techniques experience the ill effects of the accompanying two drawbacks:

(1) The strategies utilize the evaporation of carbon source that takes after a unclear way to scale up the generation with industrial standard and

(2) The CNTs produced by vaporization strategy get blended with deposits of carbon. Hence, it is very hard to purify, control, and gather CNTs for building nanotube gadget designs for practical applications.

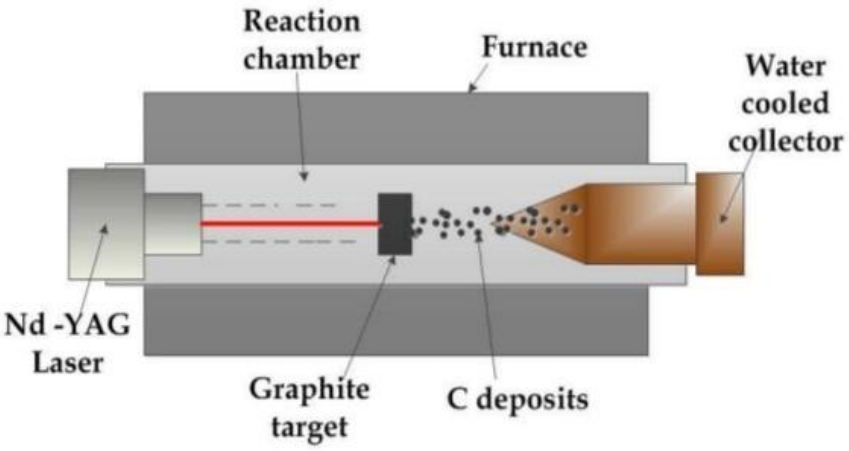

Fig 5: Laser Ablation Method

[Nanostructured materials VIII Engineering week for an intelligent ecosystem, September 2014]

2.4.3 Chemical Vapor Deposition

From last two decades, carbon fibers and filaments are synthesized utilizing chemical vapor deposition of hydrocarbons in addition to a metal catalyst. In this procedure, substantial quantity of CNTs is synthesized by catalytic CVD of acetylene over cobalt and iron. Utilizing the carbon/zeolite catalyst, fullerenes and groups of SWNTs can be synthesized along with the MWNTs. For the formation of SWNTs/MWNTs from ethylene, a lot of research work has been carried on that is supported by the catalysts such as iron, cobalt, and nickel. The late research works have additionally shown the generation of SWNTs and DWNTs on molybdenum and molybdenum–iron alloy catalyst. A dainty alumina template with or without nickel catalyst is accomplished utilizing the CVD of carbon with the pores. Ethylene can be utilized with reaction temperatures of 545ºC for Nickel catalyzed CVD and 900ºC for an uncatalyzed procedure that manufactures carbon nanostructures with open ends. Methane can likewise be utilized as carbon source for synthesizing. High yields of SWNTs at 1,000ºC are produced by catalytic decomposition of H2/CH_4 above cobalt, nickel, and iron. The use of H2/CH4 environment

between a non-reducible oxide, for example, Al_2O_3 or $MgAl_2O_4$ and one or more transition metal oxides can create the composite powders containing uniformly scattered CNTs. Consequently, higher extents of SWNTs and lower extents of MWNTs can be accomplished utilizing the decomposition of CH4 over the newly formed nanoparticles.

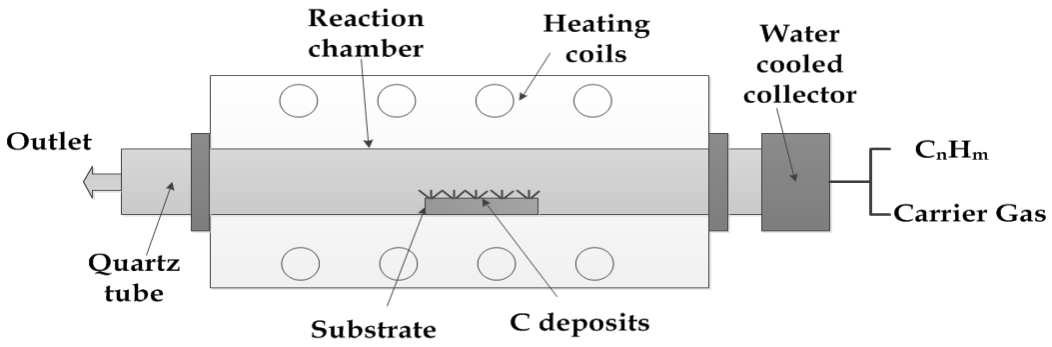

Fig 6: Chemical Vapor Deposition Method

[Kumar, Mukul, and Yoshinori Ando. "Chemical vapor deposition of carbon nanotubes: a review on growth mechanism and mass production." *Journal of nanoscience and nanotechnology* 10.6 (2010): 3739-3758]

2.5 Using Plasma for synthesis of CNTs

Laser ablation, arc discharge and chemical vapor deposition (CVD) are the methods which are generally used to synthesize CNTs. Among these, chemical vapor deposition (CVD) methods offer the greatest potential for extensive scale and commercially viable synthesis of assembled CNTs. CVD techniques have likewise been generally utilized as a part of ICs producing and in this way existing facilities are appropriate for CNT growth.

Nevertheless, the synthesis of CNTs utilizing CVD technique requires undesirably high temperature, which harms the electronic chip. A milder synthesis condition is required. Plasma-enhanced chemical vapor deposition (PECVD) technique offers an answer for low temperature production of CNTs. Similarly, PECVD strategies are additionally utilized as a part of ICs fabricating for the development of oxide and nitride thin film and its change for CNT development won't be a noteworthy issue. It is utilized to store materials like astounding Silicon

dioxide and films can be deposited at low temperatures. Plasma is a key portion of this procedure and this is the reason it is called plasma enhanced.

PECVD strategies incorporate free standing, individual and vertically aligned (VA) CNTs. This one of a kind component recognizes PECVD from CVD and opens up the likelihood of making nanodevices in light of single strand CNT. Change in catalyst support design, PECVD reactor setup, plasma conditions and synthesis parameters altogether bring down the CNT combination temperatures to 400–500°C. The PECVD strategies additionally offer the chance to change the properties of CNTs utilizing plasma and make new hybrid materials [7].

In PECVD, a cleaned substrate (essentially silicon) is coated with a metal that act as an catalyst for CNT growth, for example, Ni, Fe, Co, utilizing different deposition techniques. The coated specimens are put onto a heating plate in the center of the PECVD reactor, which is then pumped down to a low base pressure (~1mTorr) to empty atmospheric gasses. At that point the substrate is warmed to a temperature appeared to deliver carbon nanotubes (approx. 450 to 700°C). The carbon-containing and reacting gasses are brought into the chamber through a system of mass flow controllers permitting to manage the flow rate and gas composition of the mixture. Plasma is formed when a high voltage is applied across the electrode above the sample. The decomposition of the gas is caused into its components because of the energy from heating the substrate and the high voltage plasma. The definite development component of CNT arrangement is not absolutely known, in any case it is likely that carbon from the precursor gas disintegrates in the catalyst until it is supersaturated, and soon thereafter the carbon is precipitated out of the catalyst in the form of carbon nanotube. The PECVD strategy takes into consideration to control growth parameters to impact growth rate and diameter. The two most vital components of this procedure are catalyst dependency and applied electric field. The electric field orientation influences carbon nanotube growth alignment and CNTs which are straight and perpendicular to the surface are produced.

As we are using plasma in this process we have various advantages. One among the advantages is decomposition at low temperature which works awesome for materials which are temperature sensitive or which changes their characteristics at high temperatures. In plasma a specific amount of electrons are free due to partial ionization of gases, thus leaving atoms with

positive and negative charges. In this manner, it responds extremely well to electromagnetic fields. Plasma has diverse qualities of solids, fluids, and gasses and consequently plasma is considered as discrete state of matter. Plasma does not have a fixed shape or volume unless it is encased by a container. But, unlike a gas, it is enormously affected by a magnetic field.

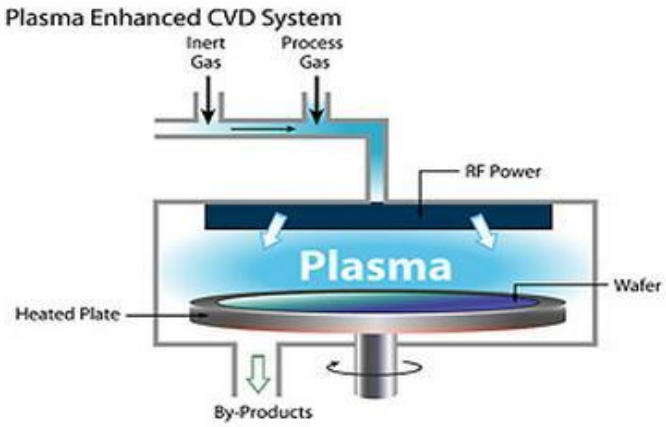

Fig 7: Plasma Enhanced Chemical Vapor Deposition Method

[Chemical Vapor Deposition Reactors, Encyclopedia of chemical engineering equipment] (http://encyclopedia.che.engin.umich.edu/Pages/Reactors/CVDReactors/CVDReactors.html)

The PECVD procedure utilizes an electrical energy to make a glow discharge which is plasma; subsequently the energy is moved into a gas mixture. Plasma is accomplished by having a Radio frequency in the AC range discharge in between two electrodes. The gases which are present in the space between electrodes use RF energy to ionize and in this way changing the different gasses that are in the PECVD chamber into reactive radicals, ions, neutral atoms and molecules. The substrate can be maintained at low temperatures as the formation of reactive and energetic species happens in the gas phase by collision. The wafers lie on a grounded aluminum plate, which serves as the base electrode for setting up the plasma. The second electrode is situated at close vicinity to the wafers. The PECVD procedure is generally utilized as a part of the produces in depositing thin films on semiconductors with temperature-sensitive structures. It can be utilized for deposit materials including Silicon Nitride, Silicon Oxide, Silicon Dioxide, Silicon OxyNitride, Diamond like Carbon, Amorphous Silicon, and Poly Silicon. At low pressure from a few hundred milliTorr to a few Torr, silicon dioxide can be produced by the

combination of silane and oxygen. Silicon nitride can likewise be formed with silane and ammonia in similar fashion. For the accumulation of Oxide, the thin film can be deposited from tetraethylorthosilicate (TEOS) with plasma. Thin films can be deposited at high deposition rate and good film stability in PECVD process which has low pressure environment and dual frequency.

In comparison with other CVD process, one of the principle advantages of PECVD is that the procedure can be carried out at low temperature while the deposition rate is practically identical to other CVD process. PECVD usually operates at low temperature (100˚C - 400˚C). The PECVD procedure utilizes both thermal energy and RF-induced glow discharge for controlling chemical reaction. Electrons which are created by glow discharge collide with reactant gases which dissociate them to initiate the reaction and hence are deposited as solid film on the substrate. Less thermal energy is required by the system as a part of energy which is use to start the chemical reaction is given by the glow discharge itself. In this manner, the temperature can be kept at relatively low level contrasting with other CVD methods.

Some other benefit of the PECVD procedure is the great properties of the films being deposited. The PECVD procedure can deposit a thin film with good dielectric properties. This is essential to ICs manufacture as the transistor require a decent dielectric layer to keep up its characteristics and execution. These films also have low mechanical stress. This can keep the films being distorted and become non-uniform as a result of the uneven mechanical stress on it. Great conformal step scope and superb consistency is provided by the PECVD procedure. The films thickness over the step edge and level surface can be made uniform. This is an extraordinary advantage of the PECVD when the manufacture procedure requires high step coverage since a portion of the manufacture procedure may have a substrate with a few steps on the surface. Despite the fact that the plasma framework makes a low temperature environment for deposition, it has its own particular disadvantage to the fabrication procedure. The plasma framework ionized the gasses and drives it to certain directions to deposit the material. The plasma gasses will collide into the surface and the plasma could harm the films. Along these lines, the gadgets may weaken amid the procedure. The other issue is that the plasma gas dependably contains hydrogen in plasma nitrides. The hydrogen inside the plasma gas can react with silicon or nitrogen to form Si-H and SiNH. This can influence numerous properties of the

gadgets including UV absorption, stability, mechanical stress, electrical conductivity, and so on [8].

2.6 Role of Heteroatoms (Doping Elements) on the growth of CNT

Due to high aspect ratio, high chemical stability and thermal conductivity, carbon nanotubes (CNTs) show fabulous electron field emission properties. In comparison to the other existing field emission devices, the field emission from CNT is viewed as the most encouraging utilization of this nanostructure on the grounds that they give high values of current density. Doping of CNTs is done by introducing an additional gas that can be nitrogen (N_2), ammonia (NH_3), boron (B), argon (Ar), hydrogen (H_2) etc. It is a viable approach to tailor the physical and chemical properties of CNTs. When CNT is doped with certain element then its radius is affected, also it affects the growth density of CNTs [9-14].

When a particular carrier gases is added to the PECVD reactor then it significantly changes the growth rate and growth density of MWNTs. This is founded by Kayastha et al. [9]. In specific, when argon is added to acetylene (C_2H_2) then it increases the growth density of multi-wall carbon nanotubes (MWNTs) whereas, on adding hydrogen and nitrogen gases, the growth density is decreased.

What are the effects on the structure and morphology of CNTs when ammonia and nitrogen is added as carrier gases was investigated by Mi et al. [10]. They found that when CNTs were grew in presence of ammonia then its diameter was larger in comparison to that in nitrogen gas. Also, ammonia grown CNTs had better alignment than that in nitrogen grown CNTs.

Jung et al. [11] explored the growth parameters in different gas situations of nitrogen, hydrogen, argon, ammonia, and their mixtures. It was additionally watched that in ammonia environment highly improved CNT growth happens than in the mixture of nitrogen and hydrogen environment.

The growth rate, growth density, and composition of MWNTs can be changed in various carrier gases; this was found by Yap et al. [12]. They examined the growth of CNT under various conditions, for example,

(a) Pure acetylene,

(b) Acetylene and argon,

(c) Acetylene and hydrogen, and,

(d) Acetylene and nitrogen.

When argon was added, it diluted the acetylene and diminishes the quantity of acetylene particles ractings on the iron (Fe) catalyst surface. The growth density of MWNTs was reduced by both nitrogen and hydrogen.

CNTs arrays has been grown on macro porous substrate by floating catalyst method in the ammonia and nitrogen carrier gases for different time, is shown by Mi and Jia [13]. They examined that the CNTs' grown in nitrogen had smaller diameters than that grown in ammonia.

Qian et al. [14] obtained the effect on size and circulation of carbon spheres when the ratio of argon to hydrogen in the carrier gas decreases. They become smaller in such condition. Likewise, pure argon supports carbon sphere's growth, whereas pure hydrogen does not.

Malgas et al. [15] examined the impact on the morphology of CNT in the presence of mixture ratios and N_2 carrier gas. They found that carbon nanotubes with smaller diameters were formed at the steady temperature of 750^0C and at higher flow rates of nitrogen.

In the present thesis, I have attempted to show the probable causes for the diverse observed behaviors of nitrogen and boron doping and its subsequent result on the growth of CNT. I have attempted to clarify the conduct of doping by means of N_2 and B through a PECVD procedure through the hydrocarbon's number density and the number density of hydrogen species made in doping gas environment and its repercussions on developing CNT.

CHAPTER III

3. THEORETICAL MODEL

Consider stainless steel reactor chamber having cylindrical shape and having a plasma source was taken. Following Denysenko et al., [16], its inner diameter was taken as (2R) = 32 cm and length (L) = 23 cm is taken into account. I have changed the number of hydrocarbons from that of Denysenko et al. [16]. They have taken a vast number of probable hydrocarbons in their theoretical modelling; however, I have limited the possible number of hydrocarbons here. Numerous possible combinations of ions in hydrogen- argon plasma has been considered by Sode et al. [17] such Ar^+, H^+, H_2^+, H_3^+, and ArH^+, yet this project considers CH_3^+, H^+, H_2, N_2 and B. Therefore, this project is hence relevant to the situations where higher hydrocarbons and differed mixtures of ions in plasma are not considered.

Here I have used different notations for the different ions. For the hydrocarbons that is the ions of methyl (CH_3), they have been denoted by 'A'; for the hydrogen ions such as H^+, H_2, the alphabet 'B' has been used to denote; and the carrier gas ions of nitrogen (N_2) and boron (B) has been denoted by 'C'. A substrate of silicon (Si) has been considered here, over which a layer of catalyst of nickel (Ni) is placed. The CH_4 gas acts as the source of carbon, in the plasma atmosphere considered here.

The throughout process is explained with the help of various equations which is given in detail. I have considered equations for

(a) Sheath equations,
(b) Charging of carbon nanotubes,
(c) Growth rate equation for electron density,
(d) Growth rate equations for the positively charged ions (which in my case are CH_3^+, H^+, N_2^+ and B^+),
(e) Growth rate equation for neutral atoms (i.e., CH_3, H_2, N_2 and B),
(f) Rate equations for energy of catalyst particle and,
(g) Equations of growth rate of the curved surface area of carbon nanotubes.

3.1 Sheath Equations

The sheath equations are given as follows, which are followed from Mehdipour et al. [18] and Lieberman and Lichtenberg [19]:

(1) The continuity equation is as follow:

$$\left(\hat{\imath}\frac{\partial}{\partial x}+\hat{\jmath}\frac{\partial}{\partial y}+\hat{k}\frac{\partial}{\partial z}\right).\hat{\imath}(n_k u_{kx}) = v_k n_e \quad \ldots (3.1)$$

(2) The ion momentum balance equation is given as:

$$m_k n_k u_{kx}\frac{du_{kx}}{dx} = e n_k E - m_k n_k v_{kn} u_{kx} \quad \ldots (3.2)$$

(3) Poisson's equation following Mehdipour et al. [18] is given as:

$$\frac{d^2\varphi(x)}{dx^2} = -4\pi\sum q_k \theta_k n_k \quad \ldots (3.3)$$

where k refers to either

(i) Electrons (e); or

(ii) CH_3^+ and H^+ ions; or

(iii) N_2^+ and B ions.

The description of various symbols is given below:

m_k = mass of the species k,

n_k = number densities of the species k,

n_e = number density of electrons,

u_{kx} = fluid velocity of the particle k,

$\varphi(x)$ = sheath potential,

v_k = ionization frequency,

v_{kn} = collision frequency with the neutrals,

q_k = charge of the species k,

θ_k = k-th ion to electron number density ratio,

$\sum_k \theta_k = 1$, and $0<\theta_k<1$ because the electron density is higher in plasma bulk than in the sheath, and

e = charge of electron.

The plasma sheath width [31] is given by:

$$\lambda_s = \frac{\sqrt{3}}{2}\lambda_d \left(\frac{2U_s}{k_B T_e}\right)^{3/4}, \quad \ldots (3.4)$$

where

$\lambda_d = \sqrt{\frac{k_B T_e}{n_e e^2}}$ is the Debye length of the plasma

U_s = substrate bias,

k_B= Boltzmann's constant, and

T_e = electron temperature.

In the present theoretical model, the ion-neutral collisions have been considered, and these collisions accomplish importance at higher pressure. On the other hand, my model did not embrace pressure impacts into record, but rather it has been accounted that with the increasing neutral pressure, the sheath width decreases.

3.2 Charging of CNT

The equation portrays the charge created on the whole CNT (i.e., hemispherical tip set over cylindrical surface), because of gradual addition of electrons and accumulation and diffusion of positively charged particles on the surface of the CNT (i.e., hemi-spherical tip over cylindrical surface).

$$\frac{dQ}{d\tau} = J_{iActs} + J_{iActcys} + J_{iBcts} + J_{iBctcys} + J_{iCcts} + J_{iCctcys} - \mu_e\left(J_{ects} + J_{ectcys}\right), \quad \ldots (3.5)$$

where

Q = charge over entire CNT, (i.e., hemi-spherical tip and cylindrical surface),

$$J_{ects} = \frac{\pi r_{CNT}^2}{2}\left(\frac{k_B T_e}{\pi m_e}\right)^{\frac{1}{2}} n_e(x) \exp\left(Q\delta_e + \frac{eU_s}{k_B T_s}\right) \quad \ldots (3.6)$$

J_{ects} = electron collection current at the surface of the hemi-spherical CNT tip,

m_e = mass of electron,

$\delta_e = \frac{e^2}{r_{CNT}\, k_B T_e}$,

r_{CNT} = hemispherical CNT tip radius,

T_s = substrate or catalyst temperature,

$$n_e(x) = n_{eo} \exp\left(\frac{|e|\varphi(x)}{k_B T_e}\right), \quad \ldots (3.7)$$

$n_e(x)$ = electron density in plasma sheath,

$$\varphi(x) = \varphi_o \exp\left(-\frac{|x|}{\lambda_d}\right), \quad \ldots (3.8)$$

$\varphi(x)$ = electrostatic potential,

φ_o = negative potential at the surface,

μ_e = sticking coefficient of electrons,

$$J_{ectcys} = n_e(x) r_{CNT} h_{CNT} \left(\frac{2\pi k_B T_e}{m_e}\right)^{\frac{1}{2}} \exp\left(\frac{eV_s}{k_B T_e} + \frac{eU_s}{k_B T_s}\right) \quad \ldots (3.9)$$

J_{ectcys} = electron collection current on the cylindrical surface of the CNT,

V_s = surface potential on the cylindrical surface of the CNT,

h_{CNT} = height of cylindrical surface of the CNT,

$$J_{ikctcys} = n_{ik}(x) r_{CNT} h_{CNT} \left(\frac{2\pi k_B T_i}{m_{ik}}\right)^{\frac{1}{2}} \left\{ \frac{2}{\sqrt{\pi}} \left(\frac{eV_s}{k_B T_i}\right)^{\frac{1}{2}} + exp\left(\frac{eV_s}{k_B T_i}\right) erfc\left[\left(\frac{eV_s}{k_B T_i}\right)^{\frac{1}{2}}\right] \right\} exp\left(-\frac{E_b}{k_B T_s}\right) exp\left(-\frac{eU_s}{k_B T_s}\right) \quad \ldots (3.10)$$

$J_{ikctcys}$ = ion collection current on the cylindrical surface of CNT,

T_i = ion temperature,

m_{ik} = mass of ions (k refers to either A, B or C positively charged ions as explained earlier),

E_b = energy barrier for bulk diffusion,

$$n_{ik}(x) = n_{iko} \left(1 - \frac{2e\varphi(x)}{m_{ik} v_i^2}\right)^{-1/2}, \quad \ldots (3.11)$$

$n_{ik}(x)$ = ion density in plasma sheath [20],

v_i = ion velocity at any point within the plasma, and

$$J_{ikcts} = \frac{\pi r_{CNT}^2}{2} \left(\frac{8k_B T_i}{\pi m_{ik}}\right)^{\frac{1}{2}} n_{ik}(x)[1 - Q\delta_i] exp\left(-\frac{E_b}{k_B T_s}\right) exp\left(-\frac{eU_s}{k_B T_s}\right) \quad \ldots (3.12)$$

J_{ikcts} = ion collection current on the hemi-spherical CNT.

$$\delta_i = \frac{e^2}{r_{CNT} k_B T_e}$$

3.3 Growth rate equation of electron density

The equation depicts the parity of electron number density in the plasma in view of dissociative ionization, recombination with ions, electron collection current, and loss of electron due to collision to the reactor walls. Following Tewari and Sharma [31], I can write

$$\frac{dn_e}{d\tau} = (\beta_A n_A + \beta_B n_B + \beta_C n_C) - (\delta_A n_e n_{iA} + \delta_B n_e n_{iB} + \delta_C n_e n_{iC}) - \mu_e n_{CNT} (J_{ects} + J_{ectcys}) \quad \ldots (3.13)$$

β_k = coefficient of dissociative ionization because of external field of the constituent neutral atoms,

$$\delta_k(T_e) = \delta_{jo}\left(\frac{300}{T_e}\right)^k \quad \ldots(3.14)$$

δ_k = coefficient of recombination of electrons and positively charged ions,
n_e = number density of electrons,
n_A = number density of neutral atom A (hydrocarbon),
n_B = number density of neutral atom B (hydrogen),
n_C = number density of neutral atom C (nitrogen and boron),
n_{iA} = number density of ion A (hydrocarbon),
n_{iB} = number density of ion B (hydrogen),
n_{iC} = number density of ion C (nitrogen and boron),
n_{CNT} = number density of CNT, and
k = constant (=-1.2) [21].

In equation (3.13) each term is accounted due to some process described below,
Ist term = rate of gain in electron density per unit time due to dissociative ionization of neutral atoms,
IInd term = decaying rate of the electron density because of the electron–ion recombination, and
IIIrd term = electron collection current at the surface of the CNT (hemi-spherical tip placed over the cylindrical surface).

3.4 Growth rate equation of positively charged ion density

Because of dissociative ionization of neutral atoms, recombination of electrons and ions, particle collection current at CNT surface, their adsorption, desorption, and thermal dehydrogenation, the following equations portray the balancing of positively charged ions in plasma. Following Tewari and Sharma [31],

$$\frac{dn_{iA}}{d\tau} = \beta_A n_A - \delta_A n_e n_{iA} - n_{CNT}\left(J_{iActs} + J_{iActcys}\right) - \varphi_{aiA} + \varphi_{desorp.iA} + \sum_i R_{i1} n_A n_{iC} \quad \ldots(3.15)$$

$$\frac{dn_{iB}}{d\tau} = \beta_B n_B - \delta_B n_e n_{iB} - n_{CNT}\left(J_{iBcts} + J_{iBctcys}\right) - \varphi_{aiB} + \varphi_{desorp\ .iB} + \varphi_{th} + \sum_i R_{i2} n_B n_{iC} \quad \ldots (3.16)$$

$$\frac{dn_{iC}}{d\tau} = \beta_C n_C - \delta_C n_e n_{iC} - n_{CNT}\left(J_{iCcts} + J_{iCctcys}\right) - \varphi_{aiC} + \varphi_{desorp\ .ic} + \sum_i R_{i1} n_A n_{iC} + \sum_i R_{i2} n_B n_{iC} \quad \ldots (3.17)$$

where

$$\varphi_{aik} = \frac{\delta P\ v}{(2\pi m_{ik} k_B T_i)^{1/2}} \quad \ldots (3.18)$$

φ_{aik} = adsorption flux over the catalyst substrate surface,

δP = partial pressure of adsorbing species [22],

ν = thermal vibrational frequency,

$$\varphi_{desorp\ .ik} = n_{ik} v\ exp\left(-\frac{E_a}{k_B T_i}\right) \quad \ldots (3.19)$$

$\varphi_{desorp\ .ik}$ = desorption flux of ions from the catalyst –substrate surface,

E_a = adsorption energy [22],

$$\varphi_{th} = n_H v\ exp\left(-\frac{E_{aTH}}{k_B T_s}\right) \quad \ldots (3.20)$$

φ_{th} = flux of type B ion (hydrogen) due to thermal dehydrogenation,

E_{aTH} = activation energy of thermal dehydrogenation,

n_H = hydrogen ion number density on the catalyst- substrate surface,

R_{i1} = rate of reaction (=1.05x10^{-10}cm^3/s) [23], and

R_{i2} = rate of reaction (=2.7x10^{-10}cm^3/s) [24].

In equations (3.15) - (3.17) each term is accounted due to some process described below:

Ist term = gain in ion density per unit time due to ionization of neutral atoms,

IInd term = electron-ion recombination,

IIIrd term = ion collection current on the surface of the CNT (hemi-spherical tip over the cylindrical surface),

IVth term = loss of ions due to their adsorption on the catalyst –substrate surface,

Vth term = gain of ion density because of the desorption of ions into plasma from the catalyst-substrate surface, and

Last term = gain in ion number density because of neutral/ion reactions [16].

In equation (3.16),

φ_{th} term = increase of hydrogen ion number density in plasma due to thermal dehydrogenation.

3.5 Growth rate equation of neutral atoms

In case of recombination of electrons and ions, dissociative ionization of neutral molecules, ion and neutral collection current over the CNT surface, the following equations explains the balance of neutral particles in plasma. Following Tewari and Sharma [31],

$$\frac{dn_A}{d\tau} = \delta_A n_e n_{iA} - \beta_A n_A + n_{CNT}(1-\mu_{iA})\left(J_{iActs} + J_{iActcys}\right) - n_{CNT}\mu_A\left(J_{Acts} + J_{Actcys}\right) - \sum_i R_{i1} n_A n_{iC} \quad \ldots (3.21)$$

$$\frac{dn_B}{d\tau} = \delta_B n_e n_{iB} - \beta_B n_B + n_{CNT}(1-\mu_{iB})\left(J_{iBcts} + J_{iBctcys}\right) - n_{CNT}\mu_B\left(J_{Bcts} + J_{Bctcys}\right) - \sum_i R_{i2} n_B n_{iC} \quad \ldots (3.22)$$

$$\frac{dn_C}{d\tau} = \delta_C n_e n_{iC} - \beta_C n_C + n_{CNT}(1-\mu_{iC})\left(J_{iCcts} + J_{iCctcys}\right) - n_{CNT}\mu_C\left(J_{Ccts} + J_{Cctcys}\right) - \sum_i R_{i1} n_A n_{iC} - \sum_i R_{i2} n_B n_{iC}\ , \quad \ldots (3.23)$$

where

$$J_{kcts} = \frac{\pi r_{CNT}^2}{2}\left(\frac{8k_B T_n}{\pi m_k}\right)^{1/2} n_k \quad \ldots (3.24)$$

J_{kcts} = neutral collection current on the surface of the hemi-spherical CNT tip,

$$J_{kctcys} = \pi r_{CNT} h_{CNT} \left(\frac{2k_B T_n}{m_k}\right)^{1/2} n_k \quad \ldots (3.25)$$

J_{kctcys} = neutral collection current on the cylindrical surface of CNT,

μ_{ik} = ion sticking coefficient (=1),

μ_k = neutral atom sticking coefficient (=1),

T_n = neutral atom temperature,

n_k = neutral atom density, and

m_k = neutral atom mass.

In equations (3.21) - (3.23) each term is accounted due to some process described below:

Ist term = gain in neutral atom density per unit time because of electron–ion recombination,

IInd term = decrease in neutral density because of dissociative ionization,

IIIrd term = gain in neutral density because of neutralization of the particles collected on the surface of the CNT,

IVth term = accretion of neutral atoms of species A and B at the surface of the CNT [21], and

Vth term = loss in number density because of neutral and ion reactions [16].

3.6 Rate equation for energy of catalyst particle

Following Tewari and Sharma [31]

$$rf\ power = C_p T_s \frac{d}{d\tau}(m_{cat})$$
$$= [J_{iActcat}\ (E_{miAc} + E_{catA}) + J_{iBctcat}\ (E_{miBc} + E_{catB}) + J_{iCctcat}\ (E_{miCc} + E_{catC})]$$
$$-\left(\frac{3k_B}{2}\right)[(1-\mu_{Ai})J_{iActcat} + (1-\mu_{Bi})J_{iBctcat} + (1-\mu_{Ci})J_{iCctcat}]T_s \quad \ldots (3.26)$$

where

$$m_{cat} = \frac{2}{3}\pi r_{cat}^3 \rho_{Ni}$$

m_{cat} = mass of catalyst particle,

r_{cat} = radius of catalyst particle,

ρ_{Ni} = mass density of catalyst particle,

C_p = specific heat of the catalyst particle (= 0.44 KJ/Kg ^oC),

$E_{catA}, E_{catB}, E_{catC}$ = ionization energies of atom A (CH_3), B (H_2) and C (either N_2 or B), respectively [21],

Here, both the substrate and catalyst temperature is assumed to be same.

$$E_{mikc}(Q) = \left(\left(\frac{(2 - Q\mu_{ki})}{(1 - Q\mu_{ki})}\right) - Q\mu_{ki}\right) k_B T_{ik} \quad \ldots (3.27)$$

$E_{mikc}(Q)$ = mean energy collected by the ions 'k' (wher k refers to ion A, B or C) at the surface of the catalyst particle [30] and,

$$\mu_{ki} = \left(\frac{e^2}{r_{cat}\, k_B T_{ik}}\right)$$

$$J_{ikctcat} = \pi r_{cat}^2 \left(\frac{8k_B T_i}{\pi m_{ik}}\right)^2 n_{ik}(x)[1 - Q\mu_{ki}] \times exp\left(-\frac{E_b}{k_B T_s}\right) exp\left(-\frac{eU_s}{k_B T_s}\right) \quad \ldots (3.28)$$

$J_{ikctcat}$ = ion collection current at the surface of catalyst particle.

While solving equation (3.26), the values considered are rf power= 100 W. At $\tau = 0$, putting $n_{iAo} = 6.72 \times 10^9 cm^{-3}, n_{iBo} = 4.48 \times 10^9 cm^{-3}, T_{io} = 2100\ K,\ T_s = 773\ K, E_b = 1.6\ eV, U_s = -50$ V and $r_{cato} = 50\ nm$ in expression for $J_{iActcat}$, $J_{iBctcat}$ and $J_{iCctcat}$, we can find $J_{iActcato}$, $J_{iBctcato}$ and $J_{iCctcato}$.

Again putting the values of $J_{iActcato}$, $J_{iBctcato}$ and $J_{iCctcato}$ along with $E_{miAc} = E_{miBc} = E_{miCc} = 13.2\ eV$, $E_{catA} = 11.87\ eV, E_{catB} = 13.7\ eV, E_{catC} = 12.21\ eV$ in equation (3.26), the radius of catalyst particle can be calculated.

The terms on the right hand side of equation (3.26) can be explained as the rate of energy transmitted to the catalyst particle because of ion accumulated at the surface of the catalyst particle due to ionization of the neutral atoms (A, B and C) present in the plasma along with the

mean energy accumulated by the ions on the catalyst surface and because of adherence of the ions to the catalyst particle site. The value of the radius for the catalyst particle at time τ is taken as the initial radius of the carbon nanotube.

3.7 Growth rate equation of the curved surface area of CNT

Following Tewari and Sharma [21]

$$r_{CNT}\frac{d(2\pi h_{CNT})}{d\tau} = \left(\left\{2n_{CH}v\,exp\left(-\frac{E_{TH}}{k_B T_s}\right) + 2S_{CH}\varphi_{iA}x_r + 2\varphi_{iA} + \frac{\varphi_{iA}\sigma_{aH}\varphi_{iB}}{v} + \varphi_c\right\}m_c + \left\{\varphi_{iA} + \frac{\varphi_{iA}\sigma_{aH}\varphi_H}{v} + \varphi_{iA}exp\left(-\frac{E_{TH}}{k_B T_s}\right)\right\}m_{iA}\right) \times \frac{D_s 2\pi r_{CNT}}{\pi r_{CNT}^2 \rho_{Ni}}\left(\frac{1}{J_{iActcys}}\right) + \mu_{CH_4}\pi r_{CNT}^2 J_{CH_4 ctcys} + \mu_c \pi r_{CNT}^2 J_{Cctcys} \quad \ldots (3.29)$$

$$\frac{d(\pi r_{CNT}^2)}{d\tau} = \left\{\varphi_{iB}exp\left(-\frac{E_b}{k_B T_s}\right) + \varphi_{iB}vexp\left(-\frac{E_{aTH}}{k_B T_s}\right) + \varphi_{iB}(1 - S_t) + \varphi_{iB} + S_{CH}\left(\varphi_{iB}x_r + v_o v\,exp\left(-\frac{\delta E_i}{k_B T_s}\right)\right)\right\}\frac{h_{CNT}(\tau)}{n_{iB}} + \mu_c \pi r_{CNT}^2 J_{Ccts} \quad \ldots (3.30)$$

where

$n_{CH} = S_{CH} v_o$

n_{CH} = number density or concentration of CH (CH denotes CH_3species) [18],

S_{CH} = surface coverages of CH_3 species [18],

v_o = number of adsorption sites per unit area [25],

E_{TH} = energy due to thermal dissociation [25],

$\varphi_{ik} = n_{ik}\left(\frac{k_B T_i}{m_{ik}}\right)^{1/2}$

φ_{ik} = ion flux of type k specis (k is either A or B),

$x_r = 2.49 \times 10^{-2} + 3.29 \times 10^{-2} E_i$

x_r = Ratio of kinetic energy associated with the motion of hydrocarbon ions impinging on the substrate to dissociation energy of CH_3 [18],

E_i = ion energy in eV (<100),

σ_{aH} = Cross section for the reactions of atomic hydrogen with adsorbed particles [18],

$$\varphi_c = \frac{n_{CH} V_{thc}}{4}$$

φ_c = ion flux of carbon ions,

$$V_{thc} = \sqrt{\frac{8T_c}{\pi m_c}}$$

V_{thc} = thermal velocity of carbon ions, T_c = temperature of carbon ions, m_c = mass of carbon ions,

$$\varphi_H = \frac{n_H V_{thH}}{4}$$

φ_H = ion flux of hydrogen ion,

$$V_{thH} = \sqrt{\frac{8T_H}{\pi m_H}}$$

V_{thH} = thermal velocity of hydrogen ions, T_H = temperature of hydrogen ions, m_H = mass of hydrogen ion,

$$D_s = D_{so} exp\left(-\frac{E_d}{k_B T_s}\right)$$

D_s = surface diffusion coefficient [25],

$D_{so} = \nu a_o^2$ = constant, a_o = interatomic distance between carbon atoms,

E_d = Energy barrier for diffusion of carbon (C) on the catalyst [25],

ρ_{Ni} = Density of nickel (Ni),

μ_{CH_4} = sticking coefficient of CH_4,

S_t = total surface coverage [18], and

δE_i= energy due to thermal decomposition of hydrocarbon ions [25].

From equations (3.29) and (3.30) the growth of the CNT over the catalyst nanoparticles can be traced. Eq. (3.29) gives the height of the cylindrical CNT surface (h_{CNT}) in which the development of cylindrical part of the CNT and the estimation of the height of the cylindrical

shaped CNT surface at a given time τ is then put into Eq. (3.30) to find the radius of hemi-spherical CNT tip (r_{CNT}). Equation (3.30) particularly computes the curved surface region of the hemi-spherical CNT tip. It determines just for the nanoparticle tip radius as base region is previously computed by the catalyst nanoparticle as they start nanoparticle growth on them.

CHAPTER IV

4. RESULTS

In this work, I have examined the impact of two carrier gasses (e.g. Nitrogen and Boron) on the growth of carbon nanotubes through the Plasma Enhanced Chemical Vapor Deposition (PECVD) procedure. In a PECVD procedure, the feedstock gas (e.g., CH_3) is dissociated when power is applied and the dissociated species cross through the plasma sheath subsequent to the decomposition of a hydrocarbon gas at the surface of the catalyst and mass diffusion of carbon into the catalyst particle till it saturates finally, to form CNTs.

Mostly, ions from plasma accretes inhomogeneously at CNTs developing as a forest as cited in Burmaka et al. [27]. Hence, in the present model, the inhomogeneous accumulation of ions on CNT growing in plasma medium aided by the catalyst is assumed.

There are three gases introduced in a PECVD chamber. These gases are hydrocarbon gas, carrier gas (acts as doping element), and hydrogen gas. In the present study, I have examined the impacts of doping elements on the growth of hemispherical tip CNT with cylindrical surface in plasma medium. The doping gasses are nitrogen (N_2) and boron (B).

The computations have been formed to examine the reliance of hydrocarbon number density, the height of cylindrical carbon nanotube surface, and radius of the hemi-spherical CNT tip by simultaneously solving equations (3.1) – (3.30) at proper boundary conditions via numerical calculation. The graph obtained are merged together to compare the results of these cases i.e., undoped and doped (N_2 and B).

The boundary conditions which are taken initially for the calculations are at $\tau = 0$, ion number density (n_{iA}) = 6.72 x 10^9 cm^{-3}, (n_{iB}) = 4.48 x 10^9 cm^{-3} and (n_{iC}) = 5.6 x 10^9 cm^{-3}, neutral atom density ($n_{Ao} = n_{Bo} = n_{Co}$) = 1 x 10^{15} cm^{-3}, electron number density (n_{e0}) = 1.2 x 10^{10} cm^{-3}, electron temperature (T_{eo}) = 1.2 eV, ion temperature (T_{io}) = 2150 K, neutral temperature (T_{no}) = 2040 K, mass of ion 'A' (m_{iA}) = 15 amu for CH_3^+ ion, mass of ion 'B' (m_{iB}) = 1 amu for H^+ ion, mass of ion 'C' (m_{iC}) = 28 amu for N_2^+ and 10.8 amu for B^+, mass of carbon (m_c) = 12 amu,coefficient of recombination of electrons and ions ($\delta_{Ao}=\delta_{Bo}=\delta_{Co}$) = 1.12 x 10^{-7} cm^3/s, radius of CNT (r_0) = 50 nm and density of Ni (ρ_{Ni}) = 8.908 g/cm^3.

Some of the other parameters used in the calculations are substrate temperature (T_s) = 773 K, thermal energy barrier on the catalyst surface (E_{TH}) = 1.3 eV, energy barrier for bulk

diffusion (E_b) = 1.6 eV, energy due to dehydrogenation of CH_3 (E_{aTH}) = 1.7 eV, adsorption energy (E_a) = 2.9 eV, thermal vibrational frequency (v) = 10^{13} Hz, number of adsorption sites per unit area (v_o) = 1.3 x 10^{15} cm^{-2}, inter atomic distance between carbon atoms (a_o) = 0.34 nm, energy barrier for diffusion of carbon on catalyst (E_d) = 0.3 eV, cross section for the reactions of atomic hydrogen with adsorbed particles (σ_{aH}) = 6.8 x 10^{-16} cm^2, partial pressure of adsorbing species (δP) = 2 Pa, CNT number density (n_{CNT}) = 10^6 cm^{-3}, number density of CH ion (n_{CH}) = 7 x 10^{14} cm^{-3}, number density of carbon (n_c) = 21 x 10^{12} cm^{-3}, and number density of hydrogen (n_H) = 21 x 10^{12} cm^{-3}.

The change in the number density of hydrocarbons (in cm^{-3}) can be seen in Fig. 8 for undoped, nitrogen doped and boron doped. We can see from the graph that with time the number density of hydrocarbon ions decreases. Also the decrease is more in the case of nitrogen doping, whereas in case of boron, the decrease is less compared to both the undoped condition and that when nitrogen is used as dopant material. The hydrocarbon concentration when no heteroatoms are used is similar with the boron doped case but still the decrease is more here than boron doping yet lesser than that of nitrogen doping situation.

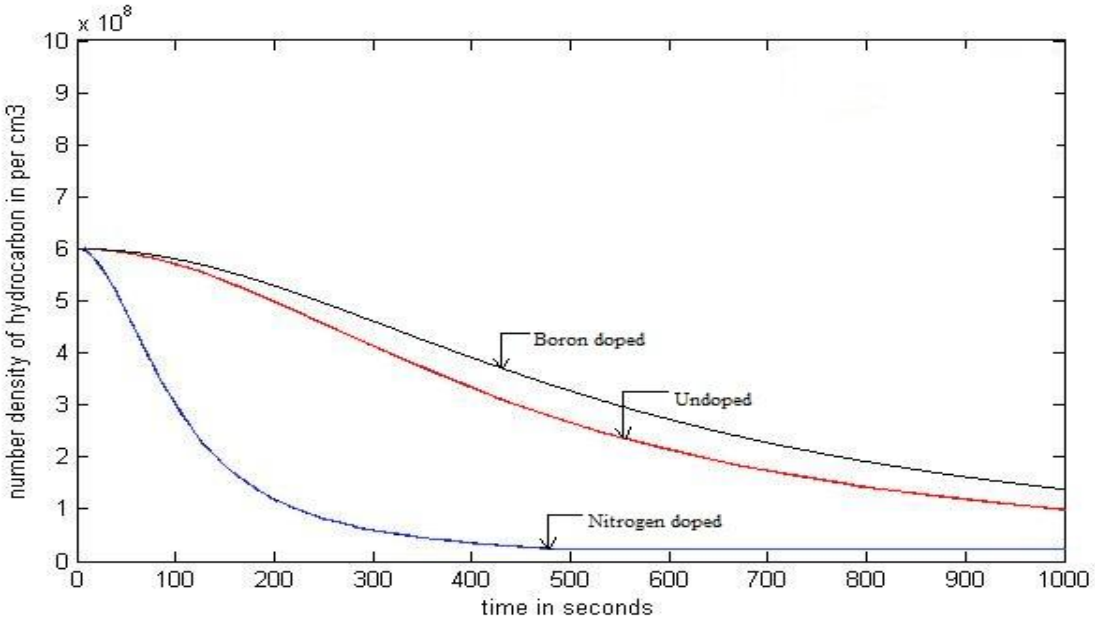

Fig.8: Time evolution of number density of hydrocarbon (in cm^{-3}) for undoped, boron doped and nitrogen doped materials.

The variation of height (in m) and radius (in m) can be seen in Fig.9 and Fig.10. Here also the comparison is done among the three conditions. The height and radius obtained for

the nitrogen gas environment is lesser compared to the other two. This can be explained as a huge number of CN radicals are formed when nitrogen is used. These radicals are volatile in nature at room temperatures and hence due to this they reduce the carbon flux which is directed to the catalyst particle thus producing lesser height as well as radius of the carbon nanotubes [28]. In case of boron the height and radius obtained are larger than in nitrogen and undoped condition. No such radicals are formed here and hence both the height and radius are larger. Whereas in undoped condition, no such gases are present hence the radius and height are larger than that in the case of nitrogen yet smaller in comparison to boron.

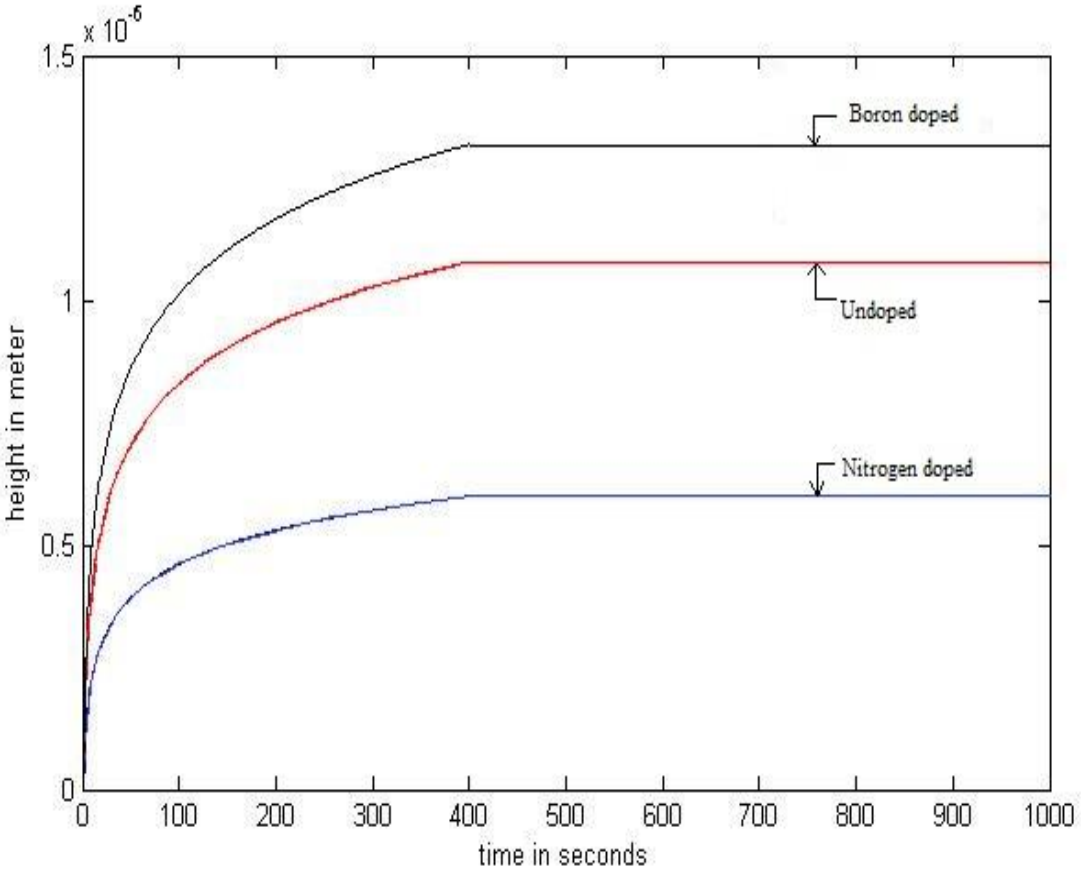

Fig.9: Time evolution of height (in m) of hemispherical tip CNT for different carrier gases N_2 and B, and also for undoped materials.

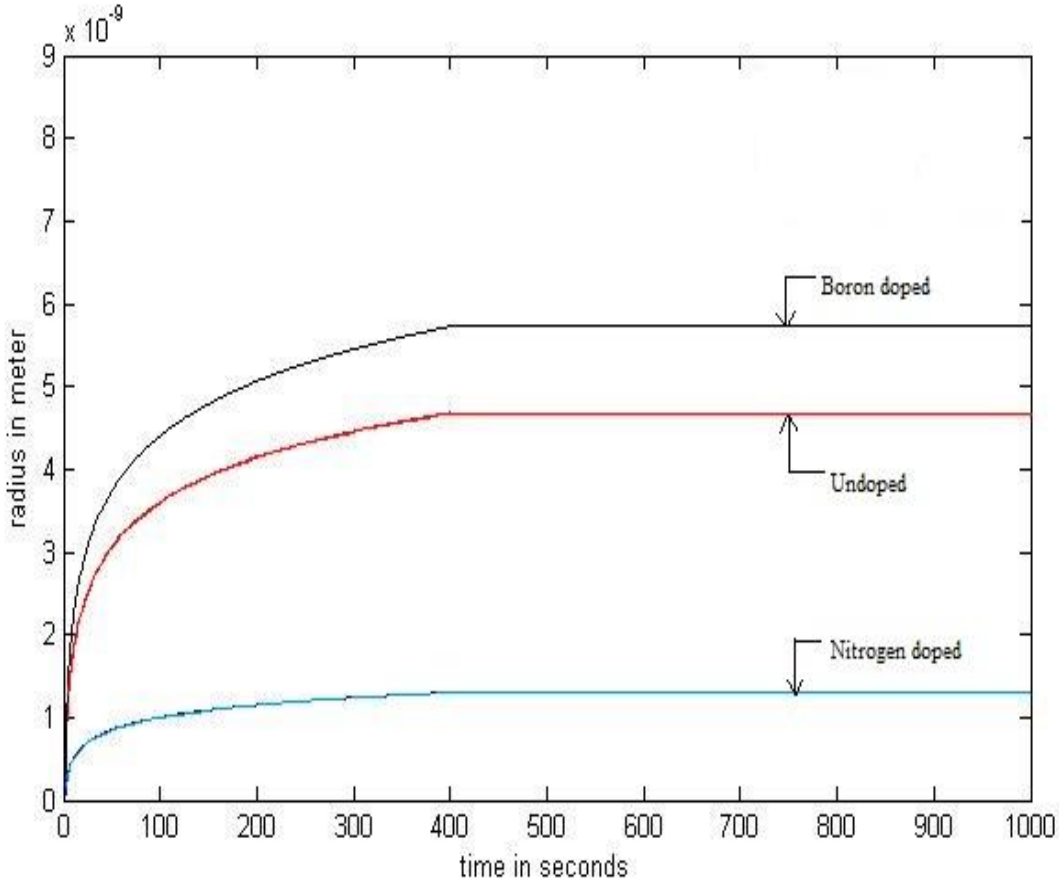

Fig.10: Time evolution of radius (in m) of hemispherical tip CNT for different carrier gases N_2 and B, and also for undoped materials.

CHAPTER V

5. CONCLUSION

The effect of two heteroatoms which are nitrogen and boron gases on the growth of the carbon nanotube is examined by a Plasma Enhanced Chemical Vapor Deposition (PECVD) procedure. For this, a theoretical model has been developed. A comparison is made for the change in height, radius and number density of hydrocarbons for the two dopant material along with the time when no heteroatoms are present for **hemispherical tip CNT with cylindrical surface**. The initial number density of neutral atoms of hydrocarbon, hydrogen and the carrier gas are assumed to be equal at 1×10^{15} cm^{-3}. Also, the ion temperature as well as the neutral temperature for hydrocarbons, hydrogen and carrier gases are assumed to be equal at 2100 K and 2000 K, respectively. The results obtained for boron is better than that of nitrogen and undoped condition.

At the point when nitrogen is taken as a dopant material, there is decrement in both height and radius of the carbon nanotube. The reason for this decrease of radius and height in the N_2 environment is that a huge number of CN radicals are formed in this environment. These radicals are volatile in nature at room temperature. Hence, this causes reduction of the carbon flux directed towards the catalyst particle, which in return causes the reduction in height and radius. But in case of boron no such radicals are formed due to which there is no hinderance in the carbon flux directed to the catalyst particle, thus the height and radius increases. Same happens when there is no dopant material. But when it is compared to the boron case then it is slightly lower than it for both radius and height. In boron rather than hindering the flux of carbon it aids to it. The same can be quoted in case of the number density of the hydrocarbon elements. Hence it can be concluded that the growth parameters are affected by the presence of a heteroatoms.

REFERENCES

[1] Asian Journal of Pharmaceutical and Clinical Research Vol.2 Issue **4**, October- December 2009 ISSN 0974-2441.

[2] M.F. Yu, B.F. Files, S Arepalli, R.S. Ruoff, Phys. Rev. Lett. **84**: 5552-5555 (2000).

[3] J.C. Charlier, X Blasé, S Roche, Rev. Mod. Phys. **79**: 677-732 (2007).

[4] A.H.C. Neto, F Guinea, N.M.R. Peres, K.S. Novoselov, A.K. Geim, Rev. Mod. Phys. **81**: 109-162 (2009).

[5] X. Wang, Qunqing Li, Jing Xie, Zhong Jin, Jinyong Wang, Yan Li, Kaili Jiang, Shoushan Fan, (2009).

[6] B. K. Kaushik and M. K. Majumder, "Carbon Nanotube Based VLSI Interconnects," Springer Briefs in Applied Sciences and Technology, 2015.

[7] Lim SanHua, Luo Zhiqiang, Shen ZeXiang, and Lin Jianyi "Plasma-Assisted Synthesis of Carbon Nanotubes Nanoscale" Res Lett. 2010; **5(9)**: 1377–1386.

[8] S. Alexandrov. Remote PECVD : a Route to Controllable Plasma Deposition. Journal de Physique IV Colloque, 1995, **05** (C5), pp.C5-567-C5-582.

[9] V. Kayastha, Y. K. Yap, S. Dimovski, and Y. Gogotsi, Appl. Phys. Lett.**85**, 3265 (2004).

[10] W. Mi, J. Y. Lin, Q. Mao, Y. Li, and B. Zhang, J. Natural Gas Chem. **14**, 151 (2005).

[11] M. Jung, K. Y. Eun, J.K. Lee, Y.J. Baik, K.R. Lee, and J. W. Park, Diamond Relat. Matter. **10**, 1235 (2001).

[12] Y. K. Yap, V. Kayastha, S. Hackney, S. Dimovski, and Y. Gogotsi, Mater. Res. Soc. Symp. Proc. **818**, M11.31.1 (2004).

[13] W. Mi and D. Jia, J. Chil. Chem. Soc **55**, 153 (2010).

[14] H.S. Qian, F.M. Han, B. Zhang, Y.C. Guo, J. Yue, and B.X. Peng, Carbon **42**, 761 (2004).

[15] G. F. Malgas, C. J. Arendse, N. P. Cele, and F. R. Cummings, J. Mater. Sci. **43**, 1020 (2008).

[16] I. Denysenko, K. Ostrikov, M. Y. Yu, and N. A. Azarenkov, J. Appl. Phys. **102**, 074308 (2007).

[17] M. Sode, T. Schwarz-Selinger, and W. Jacob, J. Appl. Phys. **114**, 063302 (2013).

[18] H. Mehdipour, K. Ostrikov, and A. E. Rider, Nanotechnology **21**, 455605 (2010).

[19] M. A. Lieberman and A. J. Lichtenberg, Principles of Plasma Discharges and Materials Processing (Wiley Interscience Publication, USA, 1994).

[20] K. Ostrikov and S. Xu, Plasma Aided Nanofabrication: From Plasma Sources to Nanoassembly (Wiley-VCH, Weinheim, Germany, 2007).

[21] A. Tewari and S. C. Sharma, Phys. Plasmas **21**, 063512 (2014).

[22] O. A. Louchev, C. Dussarrat, and Y. Sato, J. Appl. Phys. **86**, 1736 (1999).

[23] H. Chatham, D. Hils, R. Robertson, and A. C. Gallagher, J. Chem. Phys. **79**, 1301 (1983).

[24] R. L. Mills, P. C. Ray, B. Dhandapani, R. M. Mayo, and J. He, J. Appl. Phys. **92**, 7008 (2002).

[25] I. B. Denysenko, S. Xu, J. D. Long, P. P. Rutkevych, N. A. Azarenkov, and K. Ostrikov, J. Appl. Phys. **95**, 2713 (2004).

[26] C. S. Lee, B. Khang, and A. L. Barabási, Appl. Phys. Lett. **78**, 984 _2001.

[27] G. Burmaka, I. B. Denysenko, K. Ostrikov, I. Levchenko, and N. A. Azarenkov, Plasma Process. Polym. **11**, 798 (2014).

[28] Y. K. Yap, S. Kida, T. Aoyama, Y. Mori, and T. Sasaki, Appl. Phys. Lett. **73**, 915 (1998).

[29] S. K. Srivastava, A. K. Shukla, V. D. Vankar, and V. Kumar, Thin Solid Films **492**, 124 (2005).

[30] M. S. Sodha, S. Misra, S. K. Mishra, and S. Srivastava, J. Appl. Phys. **107**, 103307 (2010).

[31] Aarti Tewari and Suresh C. Sharma, Phys. Of Plasmas **22,** 043501 (2015).